NUMERICAL DYNAMIC ANALYSIS OF GEOSYNTHETICALLY REINFORCED GEOSTRUCTURES

I. Tzavara [1], Y. Tsompanakis [2], V. Zania [3], P. N. Psarropoulos [4]

[1] PhD Candidate, School of Environmental Engineering, Technical University of Crete, Chania, Greece
[2] Associate Professor, School of Environmental Engineering, Technical University of Crete, Chania, Greece
[3] Assistant Professor, Department of Civil Engineering, Technical University of Denmark, Lyngby, Denmark
[4] Post-Doctoral Researcher, School of Rural and Surveying Engineering, Technical University of Athens, Greece

---***---

Abstract - ***Geosynthetics have been widely used for various applications in engineering practice, i.e., for reinforcement, drainage, filtration, containment and separation. The development of these applications is still ongoing, not only on the evaluation of the performance, but also on expanding the applications of these advanced and continuously developing geo-engineering materials. Furthermore, in seismic prone regions, reinforcement in slopes and embankments is used to ensure slope stability against earthquake related geohazards. Various earthquakes, such as the 1999 Kocaeli and the 1999 Chi-Chi earthquakes, have demonstrated the seismic vulnerability of mechanically stabilized earth walls and reinforced slopes. Typical seismic design procedures in geotechnical earthquake engineering applications involve pseudo-static design methods. Consequently, the seismic design of reinforced geostructures does not account for several important factors, such as the compound failure and the global stability which were observed in damaged earth structures after post earthquake investigations. Thus, there is need for further investigation in this field, analytically, numerically and experimentally. Therefore, the aim of the current study is to assess the dynamic response of reinforced soil structures and the potential of the geosynthetics to prevent the development of slope instability taking advantage of their reinforcing effect. The aforementioned problem is examined numerically utilizing available experimental results of related studies. For this purpose, dynamic analyses were performed utilizing the finite element method. These analyses contribute not only to the evaluation of the dynamic response of soil reinforced structures, but also to the identification of the developed failure modes. The results of the present investigation provide a valuable insight into the seismic behavior of geosynthetic reinforced geostructures.***

Key Words: *Slope stability, Geosynthetics, Reinforcement, Seismic Response, Experiments, Numerical simulations.*

1. INTRODUCTION

Soil is a relatively inexpensive and abundant construction material, thus, it is ideal to be used for various purposes in construction of structures and infrastructures. Soil is capable of providing very high strength in compression, but practically no strength in tension. Like other construction materials with limited tensile or shear strength, soil can be reinforced with other materials to form a composite material that has increased strength. Metal strips, steel meshes and bar mats, geosynthetics and even bamboo have been used to reinforce soil (Figure 1). The first attempt to design reinforced earth structures was developed in the 1960's and the first reinforced earth retaining wall constructed in USA, using steel strips for reinforcement and was completed in 1972. Nowadays, soil reinforcement via various types of geosynthetic materials is a very popular technique used to stabilize slopes, particularly after a failure has occurred or if a steeper than a "safe" unreinforced slope is desirable. This stabilization technique can improve compaction on the edge of a slope, thus, decreasing the tendency for surface sloughing [1].

Reinforced soil structures are commonly referred to as mechanically stabilized earth (MSE) structures. Design of geosynthetically reinforced slopes is based on modified versions of classical limit equilibrium slope stability methods. Kinematically, the potential failure surface in a reinforced homogenous slope is assumed typically to be defined by the same idealized geometry (but not location) as in the unreinforced case (for example circular, log spiral, bilinear wedge). Statically, the inclination and distribution of the reinforcement tensile force along the failure surface must be postulated. The capacity of reinforcement layers is taken as either the allowable pull-out resistance behind the potential failure surface or as its allowable design strength, whichever is less. The target factor of safety for a reinforced slope is the same as for an unreinforced slope [2].

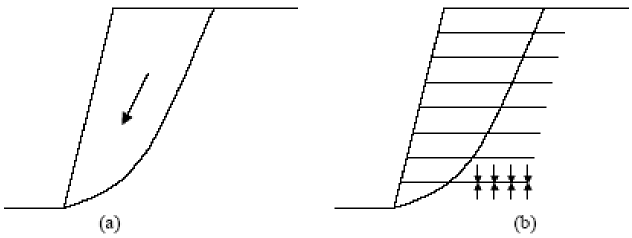

Fig -1: Schematic diagram of an unreinforced (a), and a geosynthetically reinforced slope (b)

The most common approaches for seismic stability analyses of geosynthetic reinforced soil structures are based on pseudo-static limit-equilibrium methods. These methods calculate dynamic earth pressures using the Mononobe-Okabe method or a modified two-part wedge method, which are essentially the same approach that has been used for many years for the stability analysis of conventional gravity retaining wall structures, [3, 4]. In order to give reasonable predictions of wall stability, empirical reductions of dynamic forces have often been employed [5, 6]. "Displacement methods" that treat the failed soil mass and gravity wall structure as separate rigid bodies have been proposed to overcome the dissatisfaction with limit-equilibrium based methods applied to conventional gravity structures [4, 7, 8]. In the mid 60's Newmark's rigid-block method [9] was developed for unreinforced slopes and in the sequence it was also applied to estimate permanent wall displacement, which was considered to occur by sliding at the base of the wall and/or by pullout of the reinforcing elements causing an outward tilting of the wall face. This is similar to the methodology developed by Richards and Elms [4] for gravity retaining walls. However, this method can be expected to introduce further complications when complex materials such as rate dependent polymeric reinforcements are considered together with discrete facing elements [10].

The aim of the current study is to illustrate via numerical simulations the beneficial role of the geosynthetics in mitigating the earthquake hazard on reinforced soil slopes (see Figure 1b) to prevent the development of slope instability. For this purpose, finite element analyses are performed in order to investigate the ability of the geosynthetics to reduce the permanent deformation of the geostructure, taking into account the effect of several important parameters, such as the material of the soil and of the geosynthetics, model geometry, excitations characteristics, etc. For verification purposes, numerical models are developed utilizing available data and results from two experimental studies: (a) by Nova-Roessig and Sitar [11], who performed a series of centrifuge experiments of a symmetric reinforced sandy embankment, and (b) another series of centrifuge tests of a reinforced clay embankment by Wang et al. [12]. The results of the present investigation provide a valuable insight into the seismic behavior of geosynthetic reinforced slopes.

2. FINITE ELEMENT MODELLING

In this study elaborate dynamic numerical analyses were performed utilizing the finite element method and results were verified with experimental results from the two aforementioned experimental studies. The finite element dynamic analyses were conducted utilizing the advanced capabilities of the popular ABAQUS software [13].

2.1 Simulation of first experiment

The models developed for the numerical investigation in the first part of the current investigation are based in the corresponding ones of an elaborate experimental study by Nova-Roessig and Sitar [11]. In that study a series of dynamic centrifuge tests were performed on geosynthetically-reinforced slopes and vertical walls reinforced with metallic mesh, aiming to provide a direct estimation of the impact of the geosynthetics. Based on the prototype dimensions, the employed numerical model had a height of 7.3m and the inclination was set equal to 1H:2V, as shown in Figure 1a. Furthermore, eighteen sheets of Tru-Grid reinforcement were required to maintain a static factor of safety of 1.5 when using a backfill with relative density of 75%. The length of the reinforcements did not strongly affect earthquake-induced deformations for values between 70%H and 90%H, which is typical of field conditions. Two slopes were placed back-to-back with sufficient unreinforced soil in the middle of the embankment to allow for the independent formation of potential failure surfaces. Each slope was reinforced with eighteen layers of metallic grid strips, while the reinforcement of each slope differs by means of length. The two opposing slopes, shown in Figure 2a, are called as "north" (at the left side where the length of reinforcements was 90%H) and "south" (at the right side where the length of reinforcements was 70%H).

The model has been studied under several records for various backfill densities and reinforcements of varying stiffness and length. The results of the experimental study show that the yield acceleration is primarily a function of the backfill density. It is also stated that observed horizontal deformations were reduced by using denser backfills and stiffer reinforcements, by shaking the model with smaller intensity and shorter duration events, and by decreasing the inclination of the slope faces. Moreover, it has been found that depending on the backfill density amplification occurs even for small to medium peak base accelerations, while de-amplification occurs at greater amplitudes. In addition, densification of the backfill was observed due to seismic shaking. None reinforcement rupture has been observed in any of the tests, while the reinforcements tended to spread out deformations throughout the reinforced zone and did not allow them to localize along a discrete failure surface.

(a)

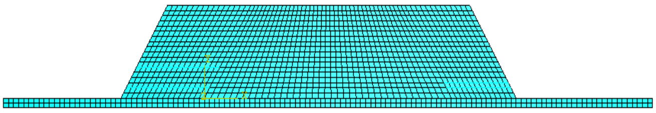

(b)

Fig -2: The model with 18 layers of reinforcement in south (right) and north (left) slope (a) and the finite element discretization (b)

In general, though the examined reinforced slopes and walls were generally under-designed by conventional pseudo-static design methods, yet no major failures were observed even after undergoing a series of intense shaking events. The results of the experimental investigation do not support the assumptions of traditional limit equilibrium-based seismic design methods. Actually, discrete failure surfaces did not form in any of the models and the models did not deform rigidly in block-like, outward motions. The slopes and walls deformed in a ductile manner under increased seismic loading, suggesting that a deformation-based seismic design method may be more applicable. Therefore, the main outcome of the experimental study was that an empirically-based approach to the evaluation of seismically-induced deformations of reinforced soil slopes and walls is feasible. The aforementioned findings of the experimental study were also verified via the present numerical analyses.

The mesh of the numerical model that corresponds to the prototype experimental configuration is shown in Figure 2b. The discretization of the backfill was performed with quadrilateral plane strain elements with size 0.5m, a mesh which is considered dense enough to produce accurate results with reasonable cost. The eighteen geosynthetic layers were placed as in the experimental setup, and were discretized with rod elements, since the geosynthetics are considered to attain only axial stiffness. Similar material properties as in the experimental study were used [11].

2.1.1 Comparison of numerical and experimental results

The dynamic analysis of the model was conducted using two of the earthquake motions applied in the experimental study, namely Gazli (1976) and Tabas (1978) records, which have quite different frequency content as shown in their response spectra in Figure 3. It has to be noted that the first period of the model (0.19s) is close to the fundamental period of the excitations. The duration of the first record was 16.28 sec, while the duration of the second record was 23.9 sec. The results in terms of accumulated deformations are shown in Figures 4a and 4b.

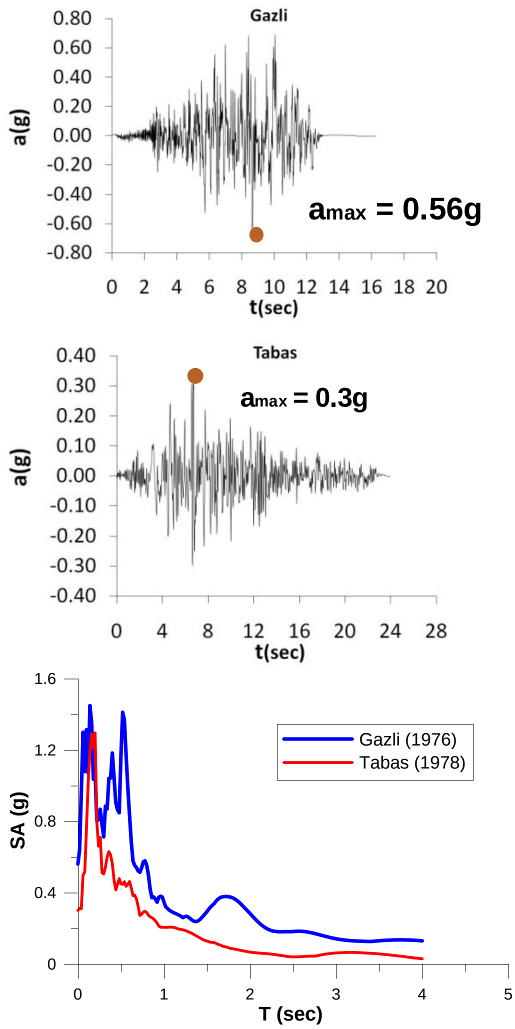

Fig -3: Time-histories and response spectra of Gazli and Tabas records

Figure 5 depicts the total displacement vectors of the south slope (with 70%H reinforcement length) for Gazli record as derived by the experimental test and the current numerical runs. Despite the differences along the height, it is evident that numerical model has captured the form of the zone of the significant deformations of the reinforced slope, i.e., the dashed straight line in Figure 5a obtained via the experimental setup. Moreover, Figures 6 and 7 depict a comparison with respect to cumulative displacements obtained numerically with the experimental ones presented by Nova-Roessig and Sitar [11]. As it can be observed, though there are certain discrepancies between the two approaches, due to unavoidable modelling variations (interface behaviour, non-linearities of the materials, etc) and numerical shortcomings to fully capture the experimental details, there is a good level of agreement regarding the behaviour of the models, since the curves have similar patterns and range of valies. In any case, numerical models were able to represent the deformation patterns of the experimental setup, where non-discrete, extensive failure zones were formed as shown in Figure 8, in which contours of plastic strains (i.e., permanent deformations) of the whole model are shown for Gazli record.

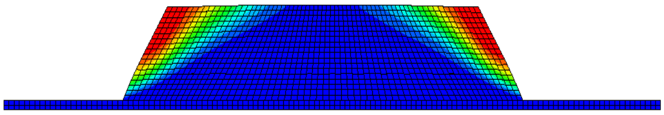

(a)

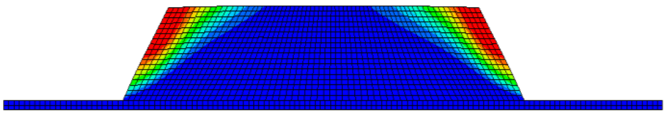

(b)

Fig -4: Contours of cumulative displacements for Gazli (a), and Tabas (b) records

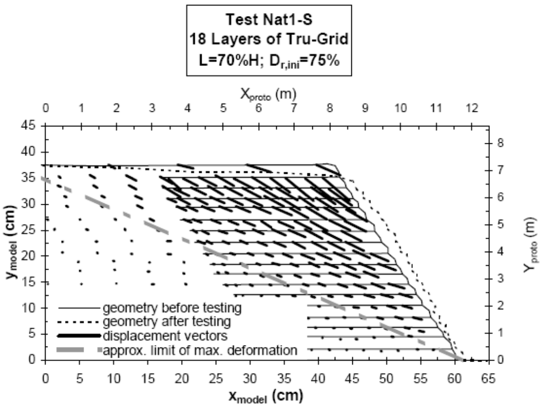

(a)

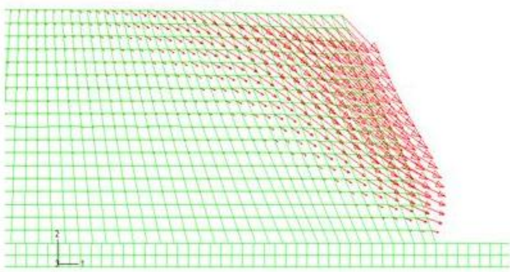

(b)

Fig -5: Total displacement vectors of the south slope for Gazli record as derived by the experimental test (a) and the numerical simulation (b)

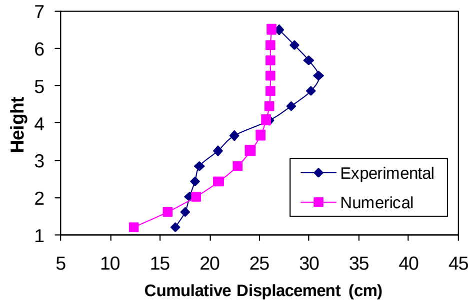

(a)

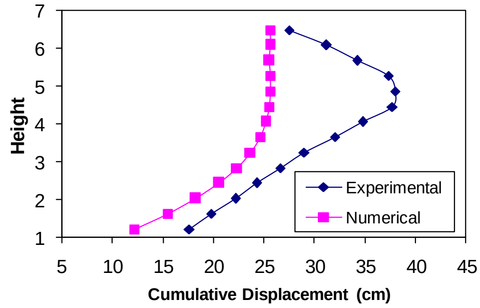

(b)

Fig -6: Contours of cumulative displacements for Gazli record for south (70%H) (a) and north (90%H) (b) sides

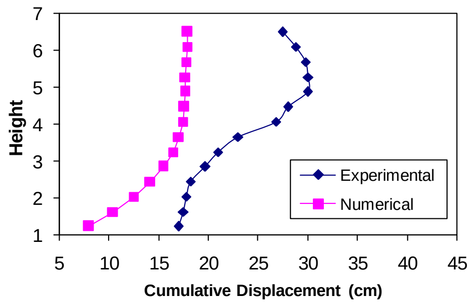

(a)

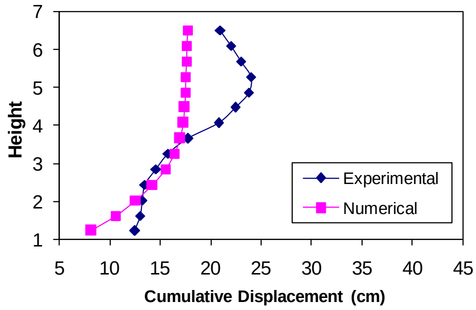

(b)

Fig -7: Contours of cumulative displacements for Tabas record for south (70%H) (a) and north (90%H) (b) sides

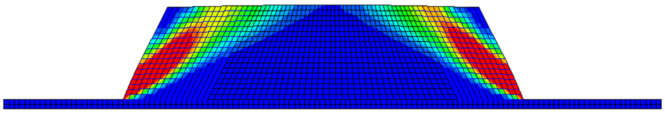

Fig -8: Contours of plastic strains for Gazli record

2.1.2 Additional numerical results

In the sequence, the numerical study was enriched using a sinusoidal pulse as base excitation, with a period of 0.288 sec having four cycles (Figure 9). Such time-histories are commonly used in dynamic analyses since the results of harmonic excitations provide a better insight to basic response characteristics, especially in analytical calculations. For instance, analytical procedures have been proposed to generate equivalent sinusoidal pulses for a big set of earthquake records and to use them in dynamic sliding analysis [14]. This pulse was scaled to two acceleration levels: 0.4g ($3.924 m/s^2$) και 0.8g ($7.848 m/s^2$).

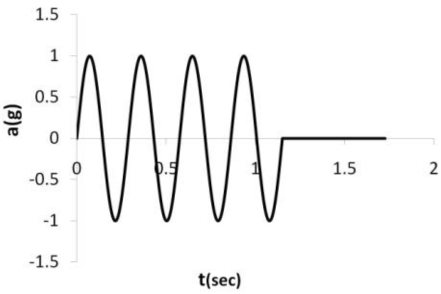

Fig -9: Sinusoidal pulse acceleration time-history

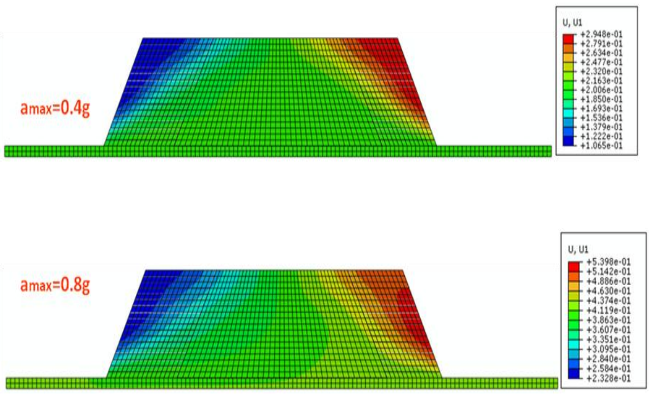

Fig -10: Accumulated horizontal displacement contours for the two levels of accelerations

Accumulated horizontal displacement contours for the two levels of accelerations are displayed in Figure 10. It can be noticed that the shape and the inclination of the triangular wedge at the reinforced regions of the geostructure is not affected much by the increase of the acceleration levels. Figure 11 depicts the accumulated plastic strain contours for the two acceleration levels, where the increase occurs (with higher values for 0.8g) at the end of each cycle of the imposed harmonic excitation as it can be seen in the time-histories of Figure 12. Finally, accelerations time-histories (for 0.4g and 0.8g, respectively) at slope toe and crest of the south (right) side of the model are shown in Figure 13. It is evident that as the acceleration levels increase, there is a minor increase in the amplification compared to lower level of seismic intensity due to the occurrence of higher plastic deformations and the resulting period elongation of the embankment.

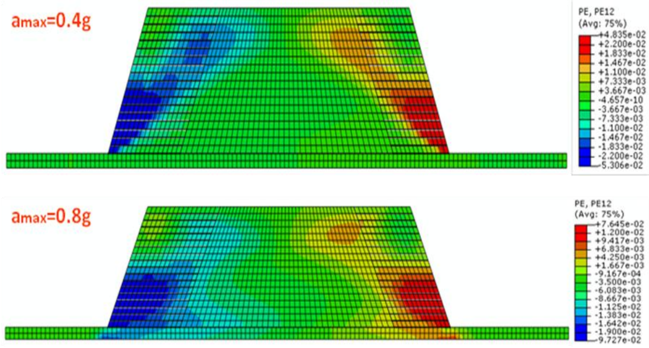

Fig -11: Accumulated plastic strain contours for the two acceleration levels

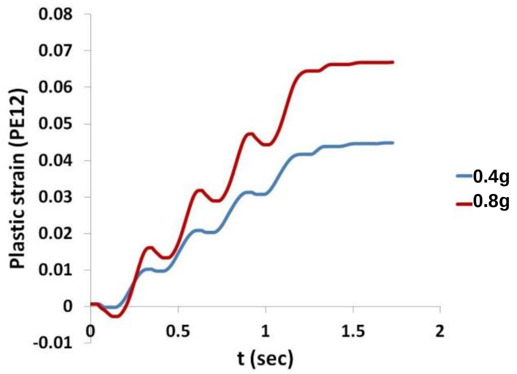

Fig -12: Time-histories of plastic strains for the two acceleration levels

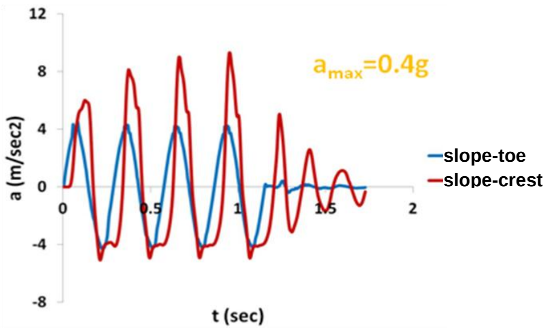

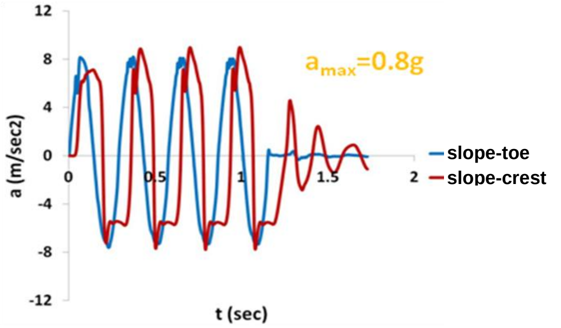

Fig -13: Acceleration time-histories for the two levels of accelerations

2.2 Simulation of second experiment

The second numerical model that has been developed for the purposes of the present numerical investigation is based on the corresponding centrifuge test of a reinforced embankment by Wang et al. [12]. In that study a series of dynamic centrifuge model tests was conducted to analyze the behavior and reinforcement mechanism of cohesive soil embankments due to seismic wave loading considering various factors that strongly influence the dynamic response and interaction between the soil and the geosynthetics. Since not sufficient details were provided in [12], the numerical simulations were not so closely developed and compared with the experimental results as in the first experimental test. The geometry of the numerical model is shown in Figure 14a, while the finite element mesh of the reinforced embankment is presented in Figure 14b having a height of 12.5m and a crest width of 2.5m. The inclination of the basic model was set equal to 1.5H:1V, while in the experiment it was also set up to 3:1 for comparison purposes. Four horizontal reinforcement layers were placed with an equal spacing of 3m. The finite element analysis of the model was performed utilizing plane strain elements for the soil and rod elements for the geosynthetics to represent their tensile stiffness. The global element size was approximately equal to 0.1m.

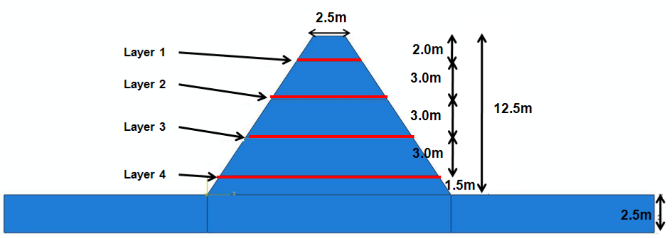

(a)

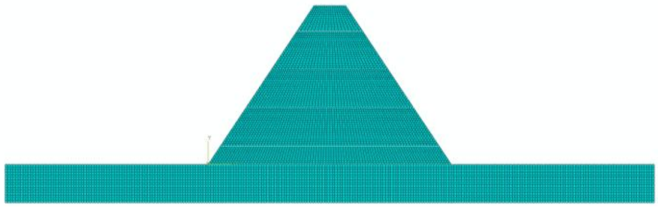

(b)

Fig -14: The model with 4 layers of reinforcement (a) and finite element discretization (b)

The main aim of this part of the numerical study was to investigate and compare the behaviour of geosynthetically reinforced embankment constructed either with cohesive soil and non-cohesive soil with typical material properties. Mohr-Coulomb failure criterion was selected to represent the yield and plastic soil behaviour with angle of friction equal to 25°, while cohesion for clay was taken as 20 kPa. In the experimental study a specific seismic wave was used [12], however, as no specific data of this time-history were provided, the parametric numerical investigation was performed utilizing the sinusoidal pulse shown in Figure 9 as base excitation of the model in Figure 14b, again scaled to two acceleration levels: 0.4g και 0.8g.

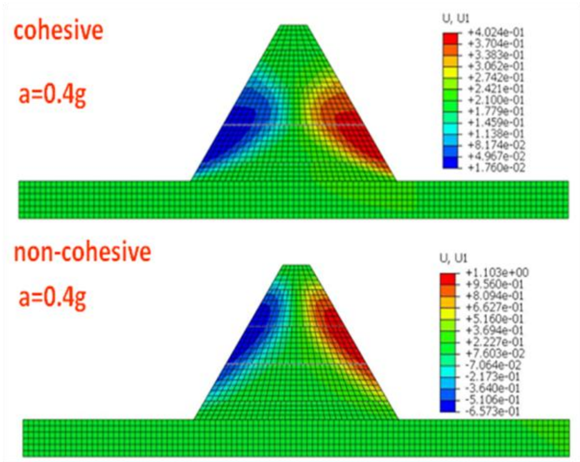

Fig -15: Permanent horizontal displacements for cohesive and non-cohesive reinforced soil

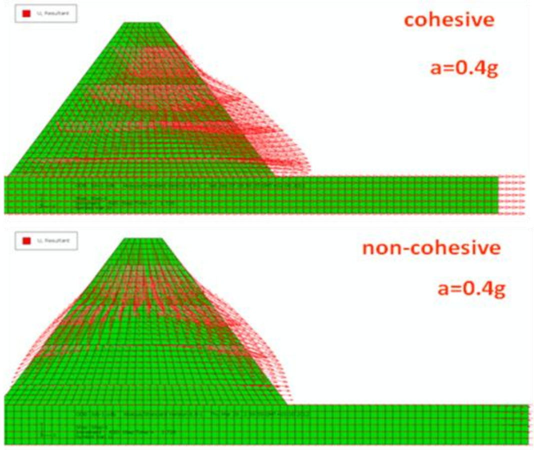

Fig -16: Total displacement vectors for cohesive and non-cohesive reinforced soil

Figure 15 shows the contours of permanent horizontal displacements at the end of the dynamic analysis for the reinforced embankment constructed with: a) cohesive (clay) and b) non-cohesive (sand) soil. The permanent displacements in both cases have a similar pattern, as it can be noticed by observing the contour plots in Figure 15. However, it is obvious that horizontal displacements are higher and more widespread for the reinforced embankment constructed by clay material. Moreover, the inclination of the failure zone is steeper in the case of the sand material, while it is also located more close to the slope crest. Analogous trends are shown in Figure 16, where a significant variation in terms of total displacement vectors can be observed between cohesive and non-cohesive reinforced soil. Finally, Figure 17 displays the contours of accumulated plastic strain contours for cohesive and non-cohesive reinforced soil, where higher and more widespread plastic strains are observed for the sandy embankment.

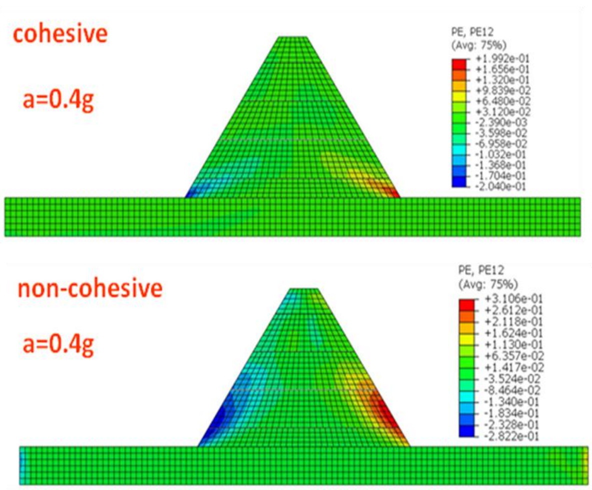

Fig -17: Accumulated plastic strain contours for cohesive and non-cohesive reinforced soil

3. CONCLUSIONS

In general, conventional pseudo-static design methods for unreinforced and reinforced geostructures adopted in seismic norms worldwide are based on crude simplifications and are unable to capture the deformation patterns of the problem at hand as it has been shown in various experimental investigations. In contrast, numerical simulations provide accurate and reliable results within the range of those obtained by similar experiments. Along these lines, it was shown in the presented investigation that, similar to experimental behavior, a discrete failure surface is not developed in finite element analyses, as a more extensive failure is observed. In other words, compared to an unreinforced slope a wider region of a reinforced earth structure is affected but to a significantly minor extent due to the presence of the reinforcement, however, this depends on the type of the soil material and other parameters.

Therefore, numerical analyses contribute not only to the more accurate evaluation of the dynamic response of reinforced geostructures, but also to the identification of the developed failure modes. Hence, they can be efficiently utilized within a framework of a displacement-based approach, in the viewpoint of contemporary performance-based design, is more reliable and realistic than conventional approaches for the evaluation of seismically-induced deformations of reinforced soil slopes and walls.

ACKNOWLEDGEMENT

This research has been co-financed by the European Union (European Social Fund - ESF) and Greek national funds through the Operational Program "Education and Lifelong Learning" of the National Strategic Reference Framework (NSRF) - Research Funding Program: Heracleitus II. Investing in knowledge society through the European Social Fund.

REFERENCES

[1] S. B. Paulsen, *A Numerical Model for Estimating Seismic Displacements of Reinforced Steep Slopes*, MSc Thesis, University of Washington, USA, 2002.

[2] L. W. Abramson, T.S. Lee, S. Sharma, and G.M. Boyce, *Slope Stability and Stabilitation Methods*, J. Wiley, 2002.

[3] H. B. Seed, and R.V. Whitman, Design of earth retaining structures for dynamic loads, ASCE Specialty Conference on Lateral Stresses in the Ground and Design of Earth Retaining Structures, Ithaca, NY, pp. 103-147,1970.

[4] R. Richards, and D. G. Elms, "Seismic behavior of gravity retaining walls", J. Geotech. Eng. Div., ASCE, Vol. 10.5, No. GT4, pp.449-464, 1979.

[5] B. R. Christopher, S. A. Gill, J. -P. Giroud, I. Juran, F. Schlosser, J. K. Mitchell, and J. Dunnicliff, *Reinforced Soil Structures*, Volume I. Design and construction guidelines, Federal Highways Administration, Washington USA, Report NO. FHWA-RD-89-043, 1989.

[6] Reinforced Earth Company, *Reinforced Earth structures in seismic regions*, Reinforced Earth Company Report, 1991.

[7] F. Nadim, and R. V. Whitman, "Seismically induced movement of retaining walls", J. Geotech. Eng., ASCE, Vol. 109, No. 7, pp. 915-931, 1983.

[8] J.-S. Lin, and R. V. Whitman, "Earthquake induced displacements of sliding blocks", J.Geotech. Eng., ASCE, Vol. 112, No. 1, pp. 44-59, 1984.

[9] N. M. Newmark, "Effects of earthquakes on dams and embankments", Geotechnique, Vol. 15, No.2, pp. 139-160, 1965

[10] Z. Cai, and R. J. Bathurst, "Seismic response analysis of geosynthetic reinforced soil segmental retaining walls by finite element method", Computers and Geotechnics, Vol. 17, pp. 523-546, 1995.

[11] L. M. Nova-Roessig, and N. Sitar, *Centrifuge studies of the seismic performance of reinforced soil structures*, Report No. UCB/GT/99-13, Dept. Civil Engineering and Environmental Engineering, University of California, Berkeley, USA, 1999.

[12] L. Wang, G. Zhang, and J. -M. Zhang, "Centrifuge model tests of geotextile-reinforced soil embankments during an earthquake", Geotextiles and Geomembranes, Vol. 29, pp. 222-232, 2011.

[13] ABAQUS, Analysis User's Manual Version 6.8.2. Simulia Inc, USA, 2010.

[14] Y., Jafarian-Manzouni, M. H. Baziar. Application of sinusoidal pulses instead of acceleration records in Newmark sliding block models. Proceedings of the 11th International Conference on Computer Methods and Advances in Geomechanics, pp. 256–72, Torino, Italy, June 19–24, 2005.